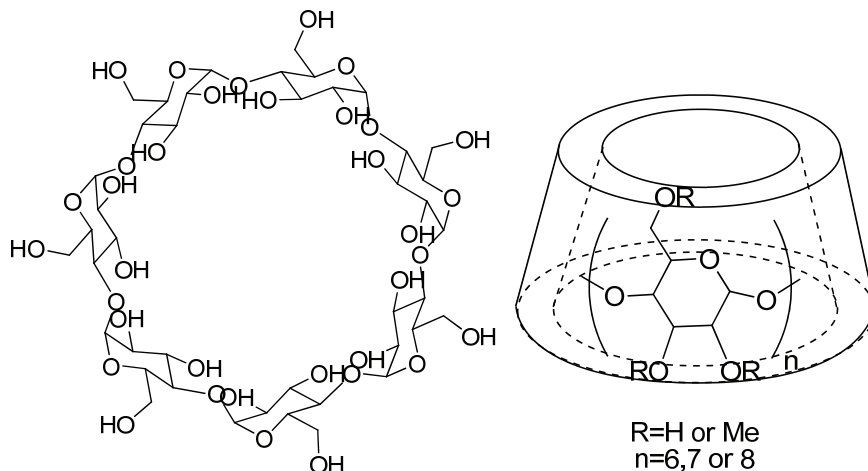


## Chapter Four: Supramolecular Structure Directing Agents *via* Adamantyl/Cyclodextrin Inclusion Complexes

### 4.1: Introduction

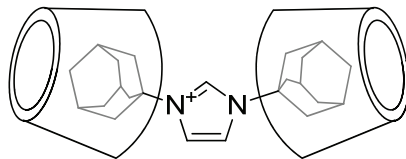
The results presented in Chapter Two using 1,3-bis(1-adamantyl)imidazolium hydroxide **15** as Structure Directing Agent (SDA) showed three crystalline phases were obtained (CIT-5 (CFI), SSZ-16 (AFX) and SSZ-35 (STF)). These results were unusual for a large, hydrophobic SDA as previous studies indicated decreasing phase diversity with increasing SDA size in high-silica reactions<sup>1</sup>. In addition, high silica reactions using SDAs with  $\Sigma(\text{C+N}) \geq 17$  have typically given one-dimensional large or extra-large pore products with relatively high framework density, e.g., SSZ-24 (AFI)<sup>2</sup>, CIT-5 (CFI)<sup>3-5</sup>, SSZ-53 (SFH), SSZ-59 (SFN)<sup>6</sup> and UTD-1 (DON)<sup>7</sup>. Synthesizing cage-based structures SSZ-16 and SSZ-35 added further distinction to the phase behavior of the bis(adamantyl) SDA. Cage-based structures are characterized by narrow windows opening into larger cavities. These materials exhibit lower framework densities compared to materials with comparable pore windows and straight pores. In addition to AFX and STF, CFI contains an undulating extra-large one dimensional pore topology with internal pockets approximately 1 nm in diameter. The apparent affinity for cage-based structures provided motivation to search for larger lobes through non-covalent assembly. If larger lobes could be created on the SDA, frameworks with increased void volume may result. Larger cycloalkyl groups were not likely to give sufficient water solubility therefore alternative SDA structure was required.

Supramolecular assemblies were created using adamantyl/ $\beta$ -cyclodextrin ( $\beta$ -CD) association complexes. CDs are cyclic oligosaccharides containing  $\alpha$ -1,4-D-glucopyranoside linked moieties. Common examples include  $\alpha$ -,  $\beta$ -, and  $\gamma$ -CD containing six, seven and eight glucose residues respectively. Larger oligomers are possible but will not be discussed here. All CDs present a hydrophilic exterior surface with primary hydroxyl groups on one face and secondary hydroxyls on the other. Scheme 4.1 shows the structure of  $\beta$ -CD ( $n=7$ ) plus a pictorial description of the three-dimensional structure. The “cup” dimensions are  $\sim 0.8$  nm high (primary hydroxyl face to secondary hydroxyl face) and 1.46 ( $\alpha$ -CD)-1.75 ( $\gamma$ -CD) nm diameter at the secondary hydroxyl face<sup>8</sup>. With all hydroxyl groups on the two planar faces CDs are water soluble and a hydrophobic cavity is created. The cavity diameter ranges from  $\sim 0.5$  ( $\alpha$ -CD) to  $\sim 0.78$  ( $\gamma$ -CD) nm with the primary hydroxyl face narrower than the secondary hydroxyl face. CD size is of similar magnitude to the cavity diameter in FAU ( $\sim 1.2$  nm) and pore diameters of 18 MR structures VPI-5 (VFI) and ITQ-33 ( $\sim 1.2$  nm)<sup>9, 10</sup>. Therefore, supramolecular assemblies containing CDs could offer exciting structures with high void volume and pore diameter.



Scheme 4.1:  $\beta$ -cyclodextrin structure and three-dimensional pictorial description

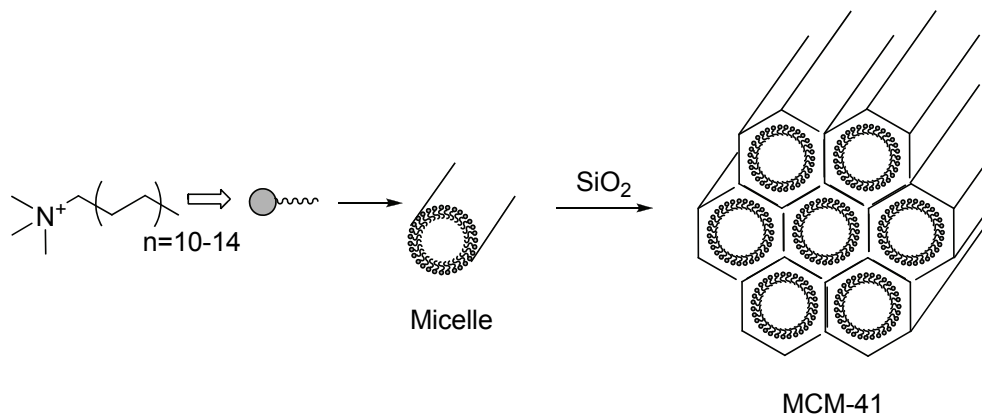
The hydrophobic cavity within each CD offers an attractive environment for inclusion complex formation. The internal diameters of  $\beta$ - and  $\gamma$ -CD are appropriate for many small molecule drugs<sup>8</sup>. Inclusion complex formation with hydrophobic drugs offers an attractive solution to limited solubility for active pharmaceutical candidates. In this context of assembling supramolecular SDAs,  $\beta$ -CD was chosen based on the strong affinity for adamantane. Scheme 4.2 illustrates the proposed 2:1 inclusion complex formed between  $\beta$ -CD and 1,3-bis(1-adamantyl)imidazolium **15**. In addition to  $\beta$ -CD, randomly methylated  $\beta$ -CD (Me-O- $\beta$ -CD) was chosen for investigation. This commercially available  $\beta$ -CD derivative contains random methoxy (CH<sub>3</sub>-O-) groups in place of hydroxyls on both faces. This derivative shows significantly higher water solubility and should offer different interactions with silicate species.



Scheme 4.2: Proposed 2:1 inclusion complex between  $\beta$ -CD and 1,3-bis(1-adamantyl)imidazolium **15**

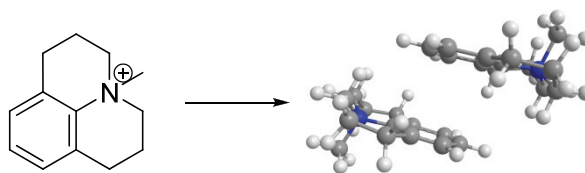
Examples of supramolecular SDAs in high-silica molecular sieve synthesis are not common. The majority of organic molecules used in molecular sieve synthesis contain nitrogen; either as an amine or quaternary ammonium moiety. Many small cyclic amines form clathrasil products such as Nonasil (NON) due to favorable van der Waals interactions. In spite of this, several novel materials were discovered using amines in conjunction with alkali hydroxide, e.g., MCM-22 (MWW) and MCM-35 (MTF) using hexamethyleneimine (homopiperidine). Water solubility/miscibility places an upper limit on the useful size of an amine for high-silica molecular sieve synthesis. In addition, alkali hydroxide incorporation to obtain sufficient silicate solubility creates competitive nucleation in solution with quartz or layered phases often produced with sufficient alkali content. In contrast, quaternary ammonium moieties convey significant water solubility and require less alkali hydroxide to obtain equivalent silicate solubility. An important consideration as the SDAs get larger (represented by  $C/N^+$ ) is where the charge is located within the molecule. Researchers at Mobil investigated increasing alkyl chain length with N,N,N-trimethylammonium headgroups and discovered the novel MCM-41S family of mesoporous silica materials<sup>11</sup>. Here was an example of supramolecular assembly leading to ordered as opposed to crystalline materials. A schematic of MCM-41 synthesis is shown

in Scheme 4.1. In light of this discovery aggregation prevention was deemed necessary as SDAs became more hydrophobic due to reduced hydrophobic hydration sphere overlap<sup>12</sup>.



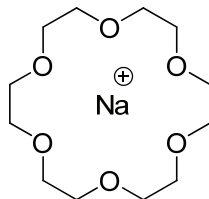
Scheme 4.3: MCM-41 formation schematic

The discussion above on avoiding uncontrolled aggregation does not preclude controlled assembly as a viable structure direction method. This was elegantly demonstrated in the recent synthesis of pure-silica Linde Type A (LTA) denoted ITQ-29<sup>13</sup>. Typical LTA materials have Si/Al~1 and the high aluminum content limits hydrothermal and acid stability. ITQ-29 synthesis uses an SDA that forms dimers in solution through aromatic  $\pi$ - $\pi$  interactions, with the SDA dimer occluded within the host product. Scheme 4.2 shows the SDA and model of the SDA dimer. This unique synthesis demonstrated controlled supramolecular assembly through non-covalent bonds as a viable tool in searching for new frameworks or novel compositions of known frameworks.



Scheme 4.4: Supramolecular SDA used to synthesize pure-silica LTA (ITQ-29)

Another example of supramolecular assembly occurs in the use of oligo-ether macrocycles (crown-ethers) with alkali cations (shown in Scheme 4.3). For this class of complex stoichiometry is restricted to one crown-ether per alkali metal cation. Gels containing 1,4,7,10,13,16-hexaoxacyloctadecane (18-crown-6) were used to synthesize EMC-2 (EMT), a structural polymorph of FAU<sup>14</sup>. Further studies investigated alkali metal/crown ether complex structure direction for FAU/EMT and concluded ion/dipole interactions directed assembly in the aluminosilicate gel<sup>15</sup>. A further example of crown-ether complex structure direction came in the synthesis of MCM-61 (MSO)<sup>16</sup>. MSO synthesis requires potassium/18-crown-6 complex as SDA. Structure solution revealed MSO contained 18 MR cavities with one crown-ether complex per cavity<sup>17</sup>. The above crown-ether-derived supramolecular SDAs are distinct from the earlier ITQ-29 dimer as ionic interactions dominate (as opposed to hydrophobic hydration interactions). This difference in structure direction does not diminish the potential application of carefully designed supramolecular assemblies in molecular sieve synthesis.



Scheme 4.5: Sodium/18-crown-6 complex

## 4.2: Experimental

1,3-bis(1-adamantyl)imidazolium hydroxide was synthesized as described in Chapter 2. In addition, 1,3-bis(1-adamantyl)imidazolium chloride was purchased from Strem Chemicals ( $\geq 97\%$ , Newburyport, MA) and was used as received.  $\beta$ -cyclodextrin ( $\beta$ -CD, Cavamax W7), randomly-methylated  $\beta$ -cyclodextrin (Me-O- $\beta$ -CD, Cavasol W7 M Pharma) and  $\gamma$ -cyclodextrin ( $\gamma$ -CD, Cavamax W8 Pharma) were purchased from Wacker Chemical Corporation (Adrian, MI) and used as received.  $\alpha$ -cyclodextrin ( $\alpha$ -CD) was purchased from Amaizo and used as received. Tetraethylammonium hydroxide (TEAOH, 35wt% aqueous solution) and polyethylene glycol ( $M_w=400$  and 3350) were purchased from Sigma-Aldrich and used as received. Inorganic reagents were used as described in Chapter Two. All inorganic reactions were performed at  $150^\circ\text{C}$  unless otherwise noted.

Inorganic reactions with adamantyl/cyclodextrin complexes were performed at CD:adamantyl molar ratios of 0.0-1.0. For example, two gels were created using 1,3-bis(1-adamantyl)imidazolium hydroxide and  $\beta$ -CD with composition 1.0  $\text{SiO}_2$ :0.029  $\text{Al}_2\text{O}_3$ :0.20  $\text{SDA}^+\text{OH}^-$ :x CD:0.25 NaOH:30.0  $\text{H}_2\text{O}$  where  $x = 0.0$  or 0.40.

Isothermal Titration Calorimetry (ITC) was performed using a MicroCal MCS instrument (Northampton, MA). Titrations were performed at 30.0°C using 1x Dulbecco's Phosphate Buffered Saline (PBS) for both guest (adamantyl) and host (cyclodextrin) solutions. Concentrations were 2.475 mM in syringe (cyclodextrin solution) and 0.1006 mM in cell (adamantyl solution). A typical experiment used 1x2  $\mu$ L injection then 10x24  $\mu$ L injections with the first 2  $\mu$ L injection discarded<sup>18</sup>. Blank experiments were performed by injecting 1xPBS into a solution of 1,3-bis(1-adamantyl)imidazolium chloride and also injecting  $\beta$ -CD solution into 1xPBS. The heat of dilution associated with each experiment was small compared to the binding enthalpy measured during the experiments, therefore, the heat of dilution was not included in the analysis. Binding stoichiometry ( $n$ ), association equilibrium constant ( $K_a$ ) and enthalpy ( $\Delta H$ ) were calculated using manufacturer supplied software. A review of the thermodynamic analysis relevant to ITC experiments using MicroCal instruments has been reported<sup>19</sup>.

N,N,N-trimethyl-1-adamantanammonium hydroxide was synthesized by quaternizing 1-adamantylamine with iodomethane using the method previously described for SDA with  $10 \leq C/N^+ \leq 14$ <sup>20</sup>. The crude iodide salt was recrystallized from hot methanol. Ion exchange to the hydroxide form was performed with Bio-Rad AG1-X8 hydroxide resin (Bio-Rad Laboratories, Hercules, CA).



### 4.3: Results and Discussion

ITC was performed using 1,3-bis(1-adamantyl)imidazolium chloride and  $\beta$ -CD. Binding stoichiometry of two cyclodextrins per bis(adamantyl)imidazolium was expected. The results are presented in Table 4.1 and a typical isotherm is presented in Figure 4.1. The results in Table 4.1 show the expected 2:1 inclusion complex was observed. The binding equilibrium constant was approximately one order of magnitude lower than reported for 1:1 adamantane/ $\beta$ -CD guest/host complexes such as 1-adamantanecarboxylic acid/ $\beta$ -CD<sup>19</sup>. The statistical analysis assumed a single binding site model with no difference between the first and second binding events. Repeating the analysis with a two site model with  $n=1$  for each site did not improve the statistical fit to the experimental data (not shown).

Table 4.1:  $\beta$ -cyclodextrin/1,3-bis(1-adamantyl)imidazolium binding stoichiometry, equilibrium constant and enthalpy

| <b>n</b>  | <b><math>K_a / M^{-1}</math></b> | <b><math>\Delta H / kJ mol^{-1}</math></b> |
|-----------|----------------------------------|--|
| 2.04±0.09 | 13900±2000                       | -23.6±1.6                                  |

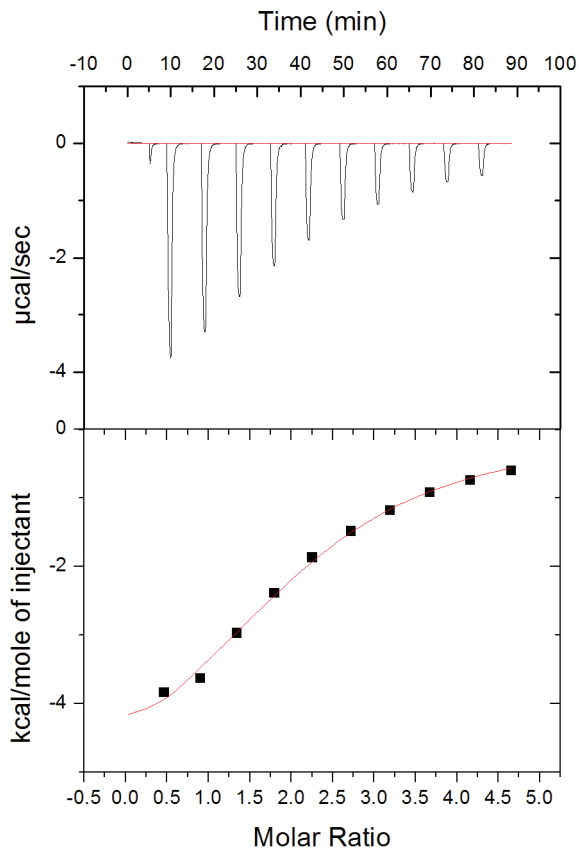


Figure 4.1: Isothermal titration calorimetry plot of 1,3-bis(1-adamantyl)imidazolium chloride/ $\beta$ -cyclodextrin guest/host complex

With experimental evidence for the desired 2:1 inclusion complex inorganic reactions were performed to investigate if the product phase could be perturbed from that obtained with 1,3-bis(1-adamantyl)imidazolium alone. The initial focus was at the moderately aluminum-rich reaction condition using NaY as aluminum source. It was anticipated that the polar, hydrophilic  $\beta$ -CD external surface would provide favorable interactions in the moderately polar aluminosilicate gel. Products from alkali metal/crown ether complexes are typically hydrophilic, with product silica to alumina (SAR) ratios of 5-8 in FAU/EMT to approximately 28 in MSO<sup>17</sup>. The results are presented in Table 4.2 and

show no perturbation with added  $\beta$ -CD or Me-O- $\beta$ -CD at NaOH/SiO<sub>2</sub>=0.25. At NaOH/SiO<sub>2</sub>=0.05, SSZ-16 was obtained when Me-O- $\beta$ -CD while addition of  $\beta$ -CD gave an amorphous product. In addition, the cyclodextrins appeared to degrade significantly under reaction conditions. All reactions with cyclodextrins gave very dark colored gels that smelled like burnt sugar. Reactions using  $\beta$ -CD appeared fluid when opened but solidified upon stirring. Therefore, no pH measurements could be made on these reactions. Figure 4.2 plots pH as a function of time for reactions involving no cyclodextrin and Me-O- $\beta$ -CD. The pH measurements for Me-O- $\beta$ -CD reactions show opposite behavior at the two sodium hydroxide concentrations studied. At the higher concentration the pH was consistently higher than the corresponding gel without CD, and even though the gel was visibly discolored pH did not decrease. In contrast, the low sodium hydroxide reaction showed a sustained pH decline over the measurement period. A sample worked-up for analysis after 10 days was amorphous with no sign of NaY reflections. Further heating lead to the formation of SSZ-16 with no residual NaY (Figure 4.3 shows XRD patterns for all three reactions at NaOH/SiO<sub>2</sub>=0.05). This suggests Me-O- $\beta$ -CD addition may offer improved product purity under certain reaction conditions.

Table 4.2: Products obtained from inorganic reactions using 1,3-bis(1-adamantyl)imidazolium hydroxide /  $\beta$ -cyclodextrin inclusion complexes. Gel compositions were 1.0 SiO<sub>2</sub>:0.029 Al<sub>2</sub>O<sub>3</sub>:0.20 SDA<sup>+</sup>OH<sup>-</sup>:x CD:y NaOH:30.0 H<sub>2</sub>O (x=0.0 or 0.40).

| Cyclodextrin      | y = 0.25  | y = 0.05  |
|-------------------|-----------|-----------|
| None              | Mordenite | SSZ-16    |
| $\beta$ -CD       | Mordenite | Amorphous |
| Me-O- $\beta$ -CD | Mordenite | SSZ-16    |

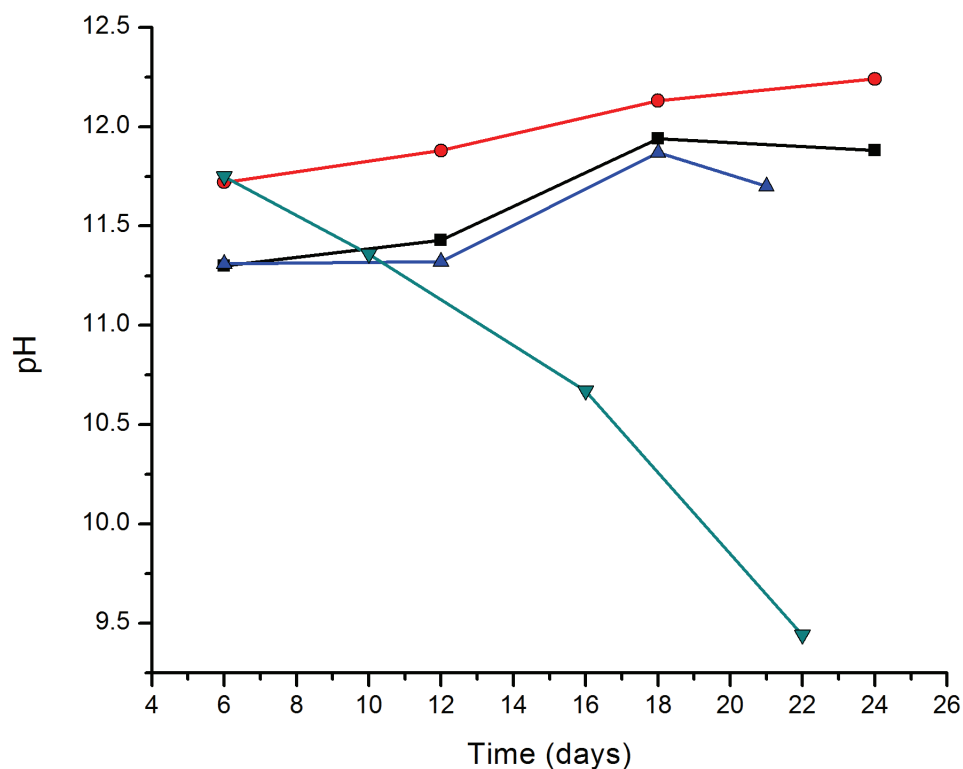


Figure 4.2: Plot of pH versus reaction time for SAR=35 reactions with no cyclodextrin and Me-O- $\beta$ -CD. NaOH/SiO<sub>2</sub>=0.25+CD/SiO<sub>2</sub>=0.0 (■), NaOH/SiO<sub>2</sub>=0.25+CD/SiO<sub>2</sub>=0.4 (●), NaOH/SiO<sub>2</sub>=0.05+CD/SiO<sub>2</sub>=0.0 (▲) and NaOH/SiO<sub>2</sub>=0.05+CD/SiO<sub>2</sub>=0.4 (▼)

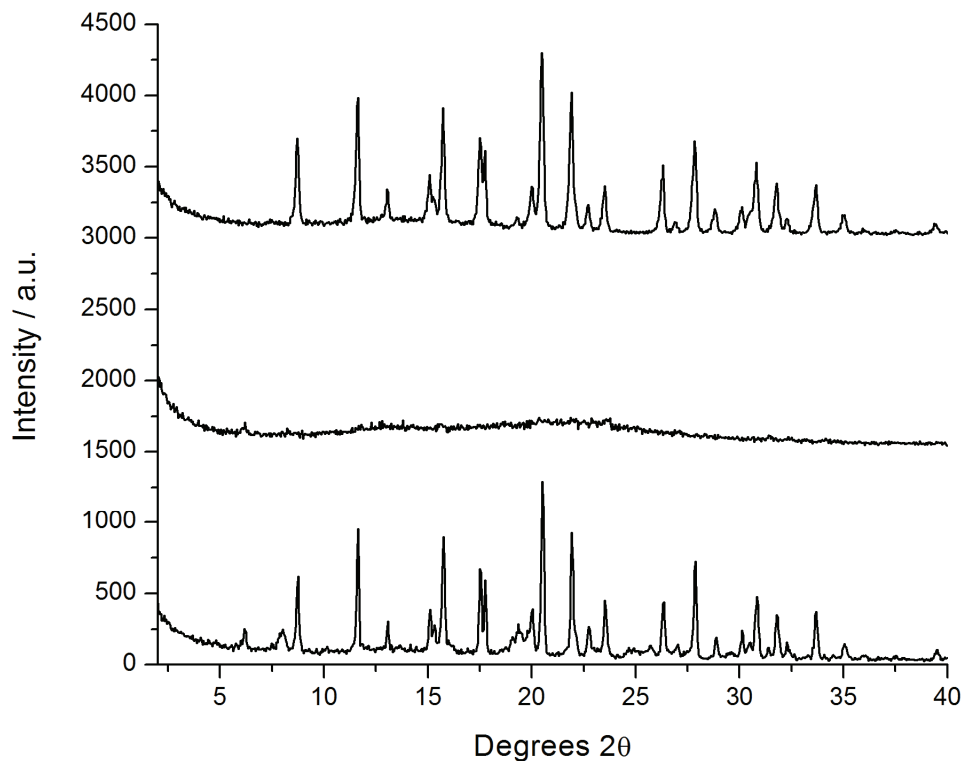


Figure 4.3: XRD patterns for 1,3-bis(1-adamantyl)imidazolium hydroxide/ $\beta$ -cyclodextrin inclusion complex. Top= Me-O- $\beta$ -CD (SSZ-16), middle =  $\beta$ -CD (amorphous) and bottom = no cyclodextrin (SSZ-16 + minor NaY)

The results from the initial inorganic reactions using bis(adamantyl)/cyclodextrin inclusion complexes did not show any desirable product perturbation. In addition, cyclodextrin degradation was significant as indicated by rapid discoloration and sustained pH decline in the low sodium hydroxide NaY reaction. The results in Chapter Two using this large bis(adamantyl) SDA suggest relatively narrow composition windows for SSZ-16, SSZ-35 and CIT-5 phases. Also, all reactions required >10 days at 150°C (or higher). The slow kinetics posed a very significant obstacle given the cyclodextrin degradation. In this regard the large bis(adamantyl) SDA must organize a large amount of silicate species

before nucleation occurs. For the STF case two cavities contain 66 tetrahedral atoms (3x10MR plus 2x18MR) so clearly a complex self-assembly process is required to coordinate adjacent silicate/organic complexes to nucleate the crystalline product. It should be noted that the final product has a lower tetrahedral atom to SDA ratio due to sharing between adjacent channels. Even accounting for this the self assembly process with such a large SDA appears very complex; adding additional size through inclusion complex formation would only increase complexity.

At this point it was not considered likely that a 2:1 inclusion complex would succeed in making a crystalline phase for the reasons outlined above. Therefore, a change to 1:1 inclusion complexes using  $\beta$ -CD and N,N,N-trimethyl-1-adamantanammonium hydroxide was made. It was anticipated that a smaller supramolecular SDA might be able to nucleate a crystalline product before significant cyclodextrin degradation occurred.

Inorganic reactions with TMADOH have been extensively studied and reported in the literature. Product phases in hydroxide reactions are largely determined by the inorganic components. With a number of products possible for a given inorganic composition multiple phases can be encountered and/or temporal evolution shows an initial product being displaced, presumably via an Ostwald ripening process<sup>21</sup>. Products obtained with this SDA include<sup>1</sup> SSZ-13 (CHA), SSZ-23 (STT), SSZ-24 (AFI), SSZ-25 (MWW), ITQ-1 (MWW)<sup>22</sup>, SSZ-31(\*STO) and VPI-8 (VET)<sup>23</sup>. These products span a wide range of lattice substitution with SSZ-13 materials often aluminum (or boron) rich (SAR~20) through to pure silica SSZ-24 and ITQ-1 (SAR= $\infty$ ). Also, rapid product formation has been reported, e.g. SSZ-13 via conversion of various faujasites in as little as 40 hours at 135°C<sup>24</sup>. In pure silica fluoride reactions CHA, STT and \*STO are observed depending on

the water to silica ratio<sup>25, 26</sup>. Similar to the hydroxide reactions, the initial products at low and high water to silica ratios are displaced upon continued heating. The initial product at  $H_2O/SiO_2 < 6$  is CHA while at  $H_2O/SiO_2 > 15$  \*STO is observed. STT displaces both phases on prolonged heating, and is the only phase observed for  $6 < H_2O/SiO_2 < 15$ <sup>27</sup>.

The inorganic reactions can be grouped into three general categories: aluminosilicate or borosilicate; zirconosilicate and miscellaneous. Representative examples are presented in Tables 4.3, 4.4 and 4.5 below. The first group contains gel compositions favorable for three-dimensional product formation with  $SiO_2/Al_2O_3$  (or  $B_2O_3$ )  $< 50$ . Both hydroxide and fluoride mediated reactions were attempted to probe cyclodextrin stability at high pH (hydroxide reactions) and approximately neutral pH (fluoride reactions). The zirconosilicate reactions were largely built around reported VET syntheses with lithium hydroxide in an attempt to obtain fast product formation<sup>23</sup>. The final group lists additional reaction attempts where no trivalent lattice element was introduced, aluminophosphate (AlPO) reaction attempts and reactions where no adamantyl component was introduced. Several reactions investigated an alternative supramolecular SDA using  $\alpha$ -CD/polyethylene glycol (PEG) threading complex. In addition,  $\gamma$ -CD was also tested in place of  $\beta$ - or Me-O- $\beta$ -CD.

Table 4.3: Aluminosilicate and borosilicate reactions employing N,N,N-trimethyl-1-adamantanammonium hydroxide (SDA<sup>+</sup>OH<sup>-</sup>) /  $\beta$ -cyclodextrin inclusion complex as structure directing agent

| Entry | Gel Composition  | Cyclodextrin      | Product          |
|-------|--|-------------------|------------------|
| 1     | 1.0 SiO <sub>2</sub> :0.1 B <sub>2</sub> O <sub>3</sub> :0.25 SDA <sup>+</sup> OH <sup>-</sup> :0.0 CD:23.0 H <sub>2</sub> O                           | None              | CHA              |
| 2     | 1.0 SiO <sub>2</sub> :0.1 B <sub>2</sub> O <sub>3</sub> :0.25 SDA <sup>+</sup> OH <sup>-</sup> :0.25 CD:23.0 H <sub>2</sub> O                          | Me-O- $\beta$ -CD | Amo+CHA          |
| 3     | 1.0 SiO <sub>2</sub> :0.02 Al <sub>2</sub> O <sub>3</sub> :0.25 SDA <sup>+</sup> OH <sup>-</sup> :0.00 CD:0.25 NH <sub>4</sub> F:10.0 H <sub>2</sub> O | None              | Amorphous        |
| 4     | 1.0 SiO <sub>2</sub> :0.02 Al <sub>2</sub> O <sub>3</sub> :0.25 SDA <sup>+</sup> OH <sup>-</sup> :0.25 CD:0.25 NH <sub>4</sub> F:10.0 H <sub>2</sub> O | Me-O- $\beta$ -CD | Amorphous        |
| 5     | 1.0 SiO <sub>2</sub> :0.02 Al <sub>2</sub> O <sub>3</sub> :0.25 SDA <sup>+</sup> OH <sup>-</sup> :0.25 CD:0.25 NH <sub>4</sub> F:10.0 H <sub>2</sub> O | Me-O- $\beta$ -CD | Amorphous        |
| 6     | 1.0 SiO <sub>2</sub> :0.02 Al <sub>2</sub> O <sub>3</sub> :0.25 SDA <sup>+</sup> OH <sup>-</sup> :0.25 CD:0.25 HF:5.0 H <sub>2</sub> O                 | $\beta$ -CD       | Amorphous        |
| 7     | 1.0 SiO <sub>2</sub> :0.02 Al <sub>2</sub> O <sub>3</sub> :0.25 SDA <sup>+</sup> OH <sup>-</sup> :0.25 CD:0.25 HF:5.0 H <sub>2</sub> O                 | Me-O- $\beta$ -CD | Amorphous        |
| 8     | 1.0 SiO <sub>2</sub> :0.10 Al <sub>2</sub> O <sub>3</sub> :0.05 SDA <sup>+</sup> OH <sup>-</sup> :0.05 CD:0.20 LiOH:30.0 H <sub>2</sub> O              | Me-O- $\beta$ -CD | Amorphous        |
| 9     | 1.0 SiO <sub>2</sub> :0.067 Al <sub>2</sub> O <sub>3</sub> :0.11 SDA <sup>+</sup> OH <sup>-</sup> :0.11 CD:1.09 NaOH:21.0 H <sub>2</sub> O             | Me-O- $\beta$ -CD | FAU <sup>a</sup> |

<sup>a</sup>Reaction performed at 90°C

Entries 1 and 2 in Table 4.3 used very similar inorganic compositions to the boron rich hydroxide reactions investigated in Chapter Two for SSZ-70. Cyclodextrin absence gave the expected B-CHA product<sup>28</sup>. In contrast, Me-O- $\beta$ -CD inclusion resulted in a mostly amorphous product with very weak CHA reflections. Figure 4.4 shows the XRD patterns for entries 1 and 2. Significant discoloration was observed with cyclodextrin incorporation where the corresponding reaction with adamantyl SDA only exhibited almost no discoloration.

The next reaction subset employed fluoride either as hydrofluoric acid or ammonium fluoride. The expectation in this series was for significantly reduced cyclodextrin degradation under the approximately neutral pH reaction conditions. Initial inspection of all reactions with cyclodextrin and fluoride addition showed black gels with a



distinct smell of burnt sugar. With rapid and significant degradation apparent the reactions were stopped after several days at 150°C.

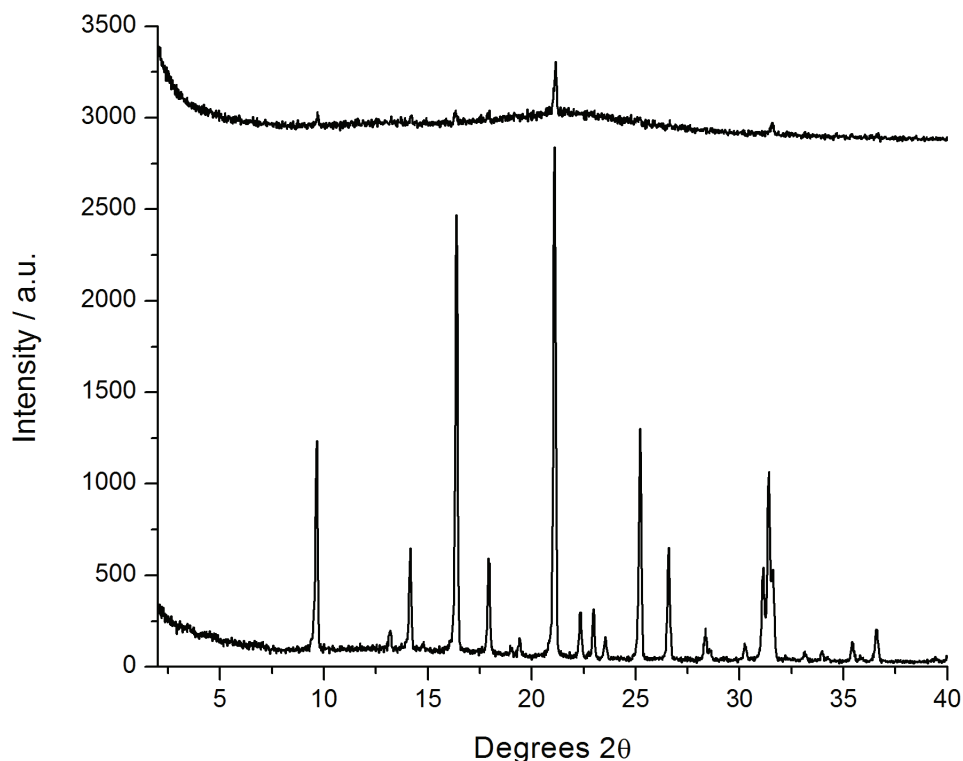


Figure 4.4: XRD patterns for borosilicate reactions employing N,N,N-trimethyl-1-adamantanammonium hydroxide/Me-O- $\beta$ -CD inclusion complex as SDA.

Top=Adamantyl SDA/Me-O- $\beta$ -CD complex (amorphous + CHA) and

bottom=Adamantyl SDA only (CHA)

The final entry in Table 4.3 represents an attempt to reduce cyclodextrin degradation by performing the reaction at lower temperature (90°C). The inorganic conditions were modeled after those used to synthesize Gmelinite (GME) using quaternary polymers<sup>29</sup>. Here the total hydroxide to silica ratio was 1.2 and silica to alumina ratio was

15. The aim was to mitigate degradation while providing enough hydroxide for silicate organization to occur. Reference 16 states FAU and P (GIS) were observed in the absence of quaternary polymer: the reaction studied above gave FAU with significant discoloration even at the lower temperature.

The reactions summarized in Table 4.3 show no desirable product perturbation. In all cases cyclodextrin degradation was significant, with fluoride addition appearing to accelerate degradation. For entries 2 and 9 crystalline phases were observed in the presence of Me-O- $\beta$ -CD. In both cases the cyclodextrin was not responsible for structure direction.

Table 4.4: Zincosilicate reactions employing N,N,N-trimethyl-1-adamantanammonium hydroxide (SDA<sup>+</sup>OH<sup>-</sup>) /  $\beta$ -cyclodextrin inclusion complex as structure directing agent

| Entry | Gel Composition   | Cyclodextrin      | Product     |
|-------|---|-------------------|-------------|
| 1     | 1.0SiO <sub>2</sub> :0.01ZnO:0.05SDA <sup>+</sup> OH <sup>-</sup> :0.00 CD:0.2LiOH:30.0 H <sub>2</sub> O                          | None              | Amorphous   |
| 2     | 1.0SiO <sub>2</sub> :0.01ZnO:0.05SDA <sup>+</sup> OH <sup>-</sup> :0.05 CD:0.2LiOH:30.0 H <sub>2</sub> O                          | $\beta$ -CD       | Amorphous   |
| 3     | 1.0SiO <sub>2</sub> :0.01 ZnO:0.05SDA <sup>+</sup> OH <sup>-</sup> :0.05 CD:0.2LiOH:30.0 H <sub>2</sub> O                         | Me-O- $\beta$ -CD | Amorphous   |
| 4     | 1.0SiO <sub>2</sub> :0.04GeO <sub>2</sub> :0.01ZnO:0.05SDA <sup>+</sup> OH <sup>-</sup> :<br>0.05CD:0.2LiOH:30.0 H <sub>2</sub> O | Me-O- $\beta$ -CD | Amorphous   |
| 5     | 1.0SiO <sub>2</sub> :0.1ZnO:0.4SDA <sup>+</sup> OH <sup>-</sup> :0.4CD:0.2LiOH:60.0 H <sub>2</sub> O                              | Me-O- $\beta$ -CD | VET         |
| 6     | 1.0 SiO <sub>2</sub> :0.04GeO <sub>2</sub> :0.05ZnO:0.3SDA <sup>+</sup> OH <sup>-</sup> : 0.3CD:0.2LiOH:45.0<br>H <sub>2</sub> O  | Me-O- $\beta$ -CD | VET+layered |

Table 4.4 summarizes representative zincosilicate reactions using TMAD<sup>+</sup>OH<sup>-</sup>/ $\beta$ -CD inclusion complexes. Entries 1–4 were run at low SDA<sup>+</sup>OH<sup>-</sup> to silica ratios in an

attempt to add just enough SDA to fully occupy the final product. Lithium hydroxide was used to supply the remaining hydroxide to give total hydroxide/silica=0.25. This total hydroxide content was sufficient in many borosilicate and aluminosilicate reactions presented in Chapters Two and Three. Entry 4 included germanium in an attempt to enhance product nucleation. Germanium incorporation often increases the population of 4MR in the product due to the longer Ge-O bond length and tetrahedral angle flexibility<sup>30</sup>. Unfortunately, no crystalline phase was obtained for all entries, presumably due to insufficient hydroxide to facilitate silicate organization in the presence of zinc.

Entries 5 and 6 were performed at higher  $\text{SDA}^+\text{OH}^-$  concentrations and VET was observed in both cases in the presence of Me-O- $\beta$ -CD. Entry 5 stands out as no evidence of layered material could be detected by XRD. Previous syntheses with  $\text{TMAD}^+\text{OH}^-$  under similar conditions gave VET plus a layered impurity<sup>31</sup>. The layered impurity appears as a relatively broad reflection at  $\sim 6^\circ 2\theta$  as shown in Figure 4.5. The absence of layered material for entry 14 further supports the observation in Table 4.2 that Me-O- $\beta$ -CD addition may improve product phase purity.

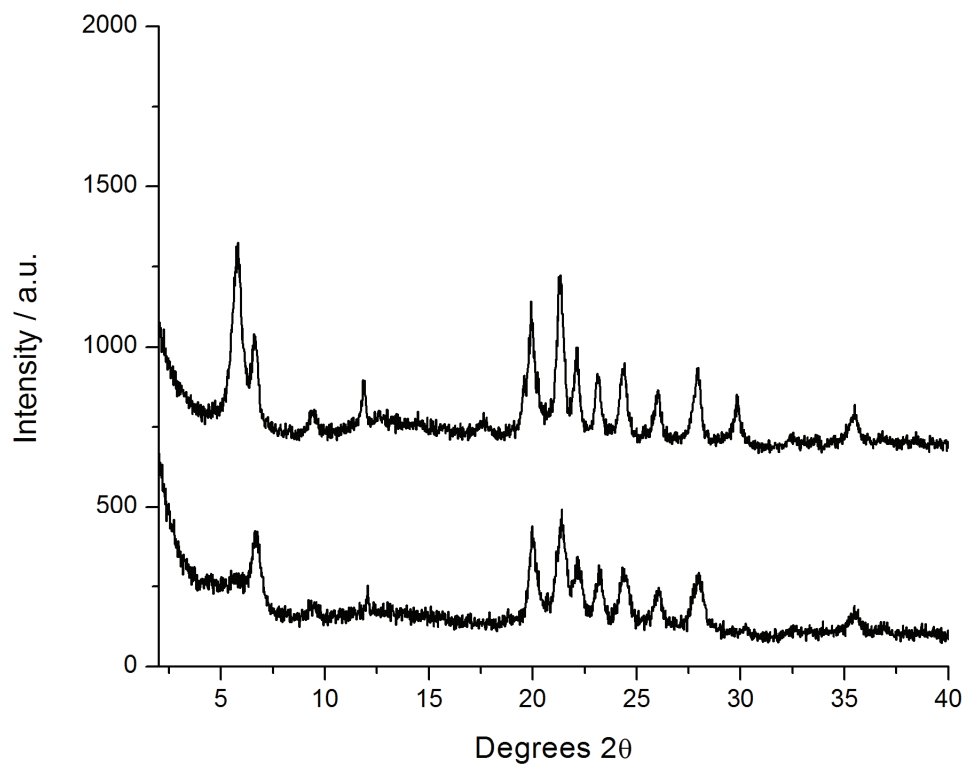


Figure 4.5: XRD patterns for zincosilicate reactions employing N,N,N-trimethyl-1-adamantanammonium hydroxide/Me-O- $\beta$ -CD inclusion complex as SDA.

Top=Adamantyl SDA/Me-O- $\beta$ -CD complex + GeO<sub>2</sub>(VET+layered) and bottom=  
Adamantyl SDA/Me-O- $\beta$ -CD complex (VET)

Table 4.5: Gel compositions and product phases for miscellaneous reactions employing cyclodextrins

| Entry | Gel Composition   | Cyclodextrin | Product                |
|-------|---|--------------|------------------------|
| 1     | 1.0 SiO <sub>2</sub> :0.04GeO <sub>2</sub> :0.30 SDA <sup>+</sup> OH <sup>-</sup> :0.00 CD:0.2LiOH:45.0 H <sub>2</sub> O              | None         | Layered+AFI            |
| 2     | 1.0 SiO <sub>2</sub> :0.04GeO <sub>2</sub> :0.30 SDA <sup>+</sup> OH <sup>-</sup> :0.30 CD:0.2LiOH:45.0 H <sub>2</sub> O              | Me-O-β-CD    | Layered                |
| 3     | 1.0 SiO <sub>2</sub> :0.10 CD:0.48NaOH:0.48HF:14.0 H <sub>2</sub> O   | α-CD         | Amorphous              |
| 4     | 1.0 SiO <sub>2</sub> :0.24 CD:0.24NH <sub>4</sub> F:14.0 H <sub>2</sub> O   | α-CD         | Amorphous              |
| 5     | 1.0 SiO <sub>2</sub> :0.24 CD:0.24NH <sub>4</sub> F:14.0 H <sub>2</sub> O   | Me-O-β-CD    | Amorphous              |
| 6     | 1.0 SiO <sub>2</sub> :0.24 CD:0.24NH <sub>4</sub> F:14.0 H <sub>2</sub> O   | γ-CD         | Amorphous              |
| 7     | 1.0 SiO <sub>2</sub> :0.3 ZnO:0.1CD:0.48NaOH:0.24HCl:20.0 H <sub>2</sub> O  | Me-O-β-CD    | Amorphous              |
| 8     | 1.0 SiO <sub>2</sub> :0.3 ZnO:0.1CD:0.48NaOH:25.0 H <sub>2</sub> O  | Me-O-β-CD    | Amorphous <sup>a</sup> |
| 9     | 1.0SiO <sub>2</sub> :0.3 ZnO:0.1CD:0.48NaOH:25.0 H <sub>2</sub> O   | Me-O-β-CD    | Amorphous <sup>b</sup> |
| 10    | 1.0SiO <sub>2</sub> :0.3 ZnO:0.1CD:0.48NaOH:25.0 H <sub>2</sub> O   | Me-O-β-CD    | Amorphous <sup>c</sup> |
| 11    | 1.0SiO <sub>2</sub> :0.1ZnO:0.06CD:0.00PEG:0.1LiOH:25.0 H <sub>2</sub> O  | α-CD         | Amorphous              |
| 12    | 1.0SiO <sub>2</sub> :0.1ZnO:0.06CD:0.01PEG <sub>400</sub> :0.1LiOH:25.0 H <sub>2</sub> O  | α-CD         | Amorphous              |
| 13    | 1.0SiO <sub>2</sub> :0.1ZnO:0.06CD:0.01PEG <sub>3350</sub> :0.1LiOH:25.0 H <sub>2</sub> O   | α-CD         | Amorphous              |
| 14    | 1.0SiO <sub>2</sub> :0.1ZnO:0.06CD:0.00PEG:0.1LiOH:25.0 H <sub>2</sub> O  | α-CD         | Amorphous <sup>d</sup> |
| 15    | 1.0SiO <sub>2</sub> :0.1ZnO:0.06CD:0.01PEG <sub>400</sub> :0.1LiOH:25.0 H <sub>2</sub> O  | α-CD         | Amorphous <sup>d</sup> |
| 16    | 1.0SiO <sub>2</sub> :0.1ZnO:0.4 TEA <sup>+</sup> OH <sup>-</sup> :0.0CD:0.2LiOH:30.0 H <sub>2</sub> O                                 | None         | VET                    |
| 17    | 1.0SiO <sub>2</sub> :0.1ZnO:0.4 TEA <sup>+</sup> OH <sup>-</sup> :0.05CD:0.2LiOH:30.0 H <sub>2</sub> O                                | Me-O-β-CD    | VET                    |
| 18    | 1.0SiO <sub>2</sub> :0.1Al <sub>2</sub> O <sub>3</sub> :0.1CD:0.48NaOH:0.48HF:14.0 H <sub>2</sub> O                                   | Me-O-β-CD    | Amorphous              |
| 19    | 0.66SiO <sub>2</sub> :0.34GeO <sub>2</sub> :0.1Al <sub>2</sub> O <sub>3</sub> :0.1CD:0.48NaOH:25.0 H <sub>2</sub> O                   | Me-O-β-CD    | AST                    |
| 20    | 0.95SiO <sub>2</sub> :0.05GeO <sub>2</sub> :0.05Al <sub>2</sub> O <sub>3</sub> :0.05CD:0.1NaOH:25.0 H <sub>2</sub> O                  | Me-O-β-CD    | Amorphous              |
| 21    | 0.98SiO <sub>2</sub> :0.02GeO <sub>2</sub> :0.03Al <sub>2</sub> O <sub>3</sub> :0.05CD:0.1NaOH:25.0 H <sub>2</sub> O                  | Me-O-β-CD    | Amorphous              |
| 22    | 1.0SiO <sub>2</sub> :0.1B <sub>2</sub> O <sub>3</sub> :0.05CD:0.1NaOH:25.0 H <sub>2</sub> O   | Me-O-β-CD    | Amorphous              |
| 23    | 1.0Al <sub>2</sub> O <sub>3</sub> :1.0P <sub>2</sub> O <sub>5</sub> :0.25SDA <sup>+</sup> OH <sup>-</sup> :0.00CD:100H <sub>2</sub> O | None         | Dense                  |
| 24    | 1.0Al <sub>2</sub> O <sub>3</sub> :1.0P <sub>2</sub> O <sub>5</sub> :0.25SDA <sup>+</sup> OH <sup>-</sup> :0.25CD:100H <sub>2</sub> O | Me-O-β-CD    | Dense                  |
| 25    | 1.0Al <sub>2</sub> O <sub>3</sub> :1.0P <sub>2</sub> O <sub>5</sub> :0.25SDA <sup>+</sup> OH <sup>-</sup> :0.25CD:100H <sub>2</sub> O | β-CD         | Dense                  |

<sup>a</sup>Reaction performed at 90°C with 4 hour periods at 135°C

<sup>b</sup>Reaction performed at 90°C with 8 hour periods at 135°C

<sup>c</sup>Reaction performed at 90°C with 4 hour periods at 150°C

<sup>d</sup>Reaction performed at 90°C

Table 4.5 provides additional inorganic reaction examples where various cyclodextrins were added to the reaction gel. Entries 1–6 contained no trivalent lattice element (aluminum or boron) in contrast to the previous syntheses outlined in Tables 4.1–4.4. With no trivalent lattice element one dimensional products (or clathrates) were expected. Entry 1 shows SSZ-24 (AFI) plus a layered impurity was obtained in a germanosilicate reaction using only  $\text{TMAD}^+\text{OH}^-$ . The same gel composition with Me-O- $\beta$ -CD gave the layered phase only. In this instance cyclodextrin incorporation lead to an undesirable phase dominating in contrast to those cases discussed above where cyclodextrin incorporation suppressed undesirable impurity phases. The high lithium hydroxide content most likely contributed to layered phase formation. No attempts were made to repeat the reactions at lower lithium hydroxide concentration.

The remaining pure silica reactions investigated  $\alpha$ - and  $\gamma$ -CD in addition to Me-O- $\beta$ -CD. As  $\alpha$ -CD could not form an inclusion complex with adamantane none was added. One reaction used NaF as fluoride source whereas the remaining reactions used  $\text{NH}_4\text{F}$ . All four examples gave amorphous products and reaction gels were dark brown to black in color when first opened. Given the severe degradation observed in all cases no insight could be gained into the relative stability of each cyclodextrin.

Entries 7–17 summarize additional zincosilicate reaction attempts with no adamantane component added. Entries 7–10 used inorganic compositions closer to those reported for VPI-7 (VSV)<sup>32</sup>. An additional aspect of these reactions was an attempt to manage cyclodextrin degradation by performing the reactions at two temperatures. For example, entry 8 used 90°C for six days then four hours at 135°C before returning to 90°C. The intention was to find a temperature where minimal degradation occurred (as evidenced

by color change) and holding at this temperature to hopefully facilitate some silicate bond rearrangement. Trial experiments revealed 90°C was the upper temperature limit for the given hydroxide to silica ratio ( $\text{NaOH}/\text{SiO}_2=0.48$ ; recall significant discoloration was observed for entry 9 in Table 4.3 at 90°C with  $\text{OH}^-/\text{SiO}_2=1.2$ ). The period at higher temperature was included to provide additional thermal energy that might induce nucleation while not long enough for significant degradation to occur. If nucleation occurred at elevated temperature crystal growth could continue at lower temperature. Entries 7, 9 and 10 showed significant discoloration (deep brown to black), whereas entry 8 was tan colored. Therefore, it did appear that degradation could be managed to some extent but ultimately no crystalline phase was obtained for all entries.

Entries 11–15 explored  $\alpha$ -CD/PEG threading complexes as alternative supramolecular SDAs. Low alkali hydroxide concentrations were used with the intention of minimizing cyclodextrin degradation. The initial reactions at 150°C gave amorphous products and significant discoloration was observed. This prompted experiments performed entirely at 90°C (entries 14 and 15) whereby discoloration was greatly reduced but again no crystalline product evolved.

The above examples where Me-O- $\beta$ -CD addition still gave SSZ-16 and VET suggested the cyclodextrin and decomposition products had a neutral to slightly positive effect on phase purity. For the SSZ-16 case a potential hypothesis was the cyclodextrin components prevented stabilization of the NaY reagent thereby giving full transformation. In contrast, the VET example suggested suppression of a competing layered phase. Entries 16 and 17 were included to further investigate the role Me-O- $\beta$ -CD addition had on phase selectivity and purity. Specifically, could Me-O- $\beta$ -CD addition effect a reaction where no

adamantyl component was added? Entry 16 represents a control experiment where tetraethylammonium hydroxide was used in a zinc-containing gel to produce VET<sup>33</sup>. Addition of Me-O- $\beta$ -CD in entry 17 did not change the product phase. This indicated the cyclodextrin decomposed and acted as a neutral species in the reaction gel.

The next reaction group summarizes reactions where no adamantyl component was added in moderately polar gels. Entry 18 was adapted from the reaction condition used by Burkett when investigating FAU/EMT structure direction using alkali metal/crown-ether complexes<sup>15</sup>.  $\alpha$ -CD was attempted with degradation noted; therefore Entry 18 was performed under approximately neutral conditions with HF addition. Significant degradation was observed for this reaction consistent with all other cyclodextrin reactions with fluoride addition. Entries 19–21 explored germanosilicate reactions with not adamantyl component added. AST was obtained at Si/Ge=2 with amorphous products at higher Ge/Si ratios. As discussed previously, AST is rich in D4R and appears frequently at low Si/Ge ratios. For the gel composition studied, aluminum incorporation could be balanced by sodium cations and this might be sufficient to stabilize the cages. Alternatively, decomposed sugar moieties could be small enough to become occluded within the cage (intact CD would be too large to fit). No structure directing role can be directly attributed to the cyclodextrin, although decomposition fragments might play a minor role with the inorganic composition largely dictating the product. The final reaction in this group explored a borosilicate reaction. Here the SiO<sub>2</sub>/B<sub>2</sub>O<sub>3</sub> was 10 and the NaOH/SiO<sub>2</sub> ratio was kept low at 0.1 to minimize degradation. At these conditions there would be insufficient positive charge to balance negative framework charge if all boron was incorporated. However, studies have shown boron tends to be drawn into the growing



crystal as required<sup>34</sup>. This offered a potential window where borate buffering could offer reduced pH and hence improved CD stability. Unfortunately, no product was obtained and discoloration was observed indicating degradation.

The final entries give details of AIPO reactions. These reactions were attempted as many AIPO products form with little or no induction period. Cyclodextrin degradation was expected under the acidic reaction conditions but if degradation was slightly slower than crystallization novel phases could evolve. The results show an unidentified dense phase was obtained for all three reactions and Figure 4.6 gives the XRD pattern. Both gels with CD added became deep black and particularly pungent smelling. It should be noted that AFI has been reported in AIPO reactions using the adamantyl SDA<sup>24</sup>. Fine tuning the gel composition should enable replication; however, severe CD degradation did not warrant further reactions.

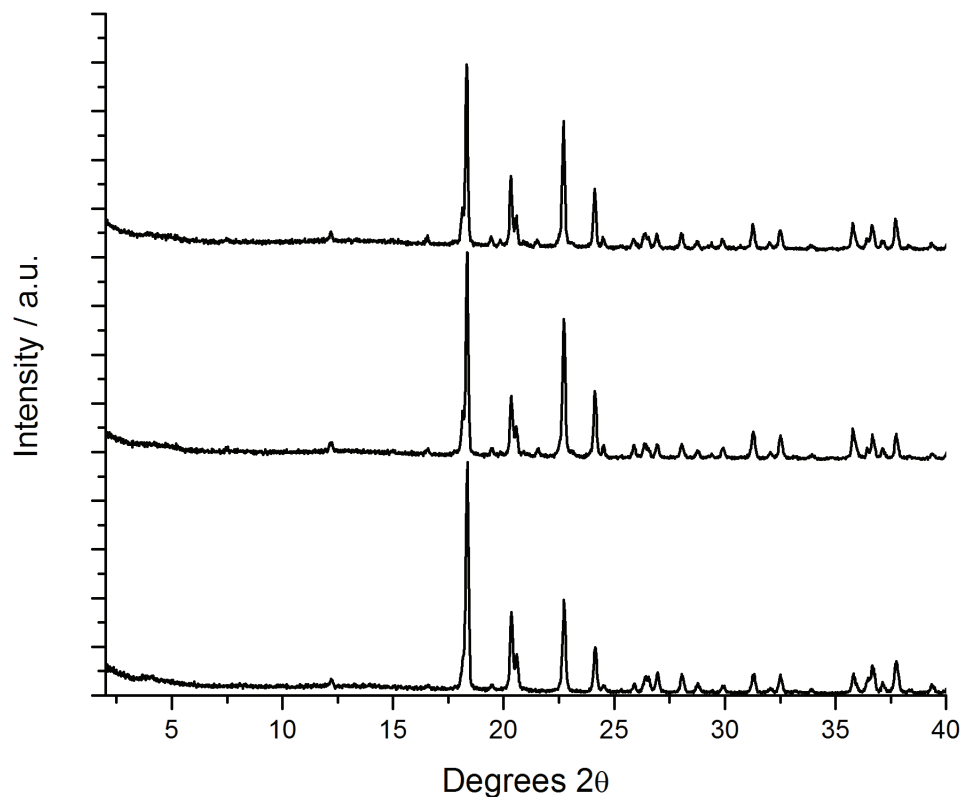


Figure 4.6: XRD patterns of unknown dense aluminophosphate phase. Top to bottom=Adamantyl SDA/ $\beta$ -CD complex, adamantyl SDA/Me-O- $\beta$ -CD and adamantyl SDA only

#### 4.4: Conclusions

Supramolecular SDAs based on adamantyl/ $\beta$ -CD inclusion complexes were not able to perturb the observed product. Inorganic reactions containing  $\beta$ -CD or Me-O- $\beta$ -CD yielded AFX, MOR, CHA, FAU, VET and AST under appropriate inorganic conditions with all remaining products amorphous or layered. No structure direction could be attributed to CD addition for any crystalline phase observed. All reactions with CD

addition performed above 90°C showed significant discoloration indicating degradation occurred. Reactions at approximately neutral pH using fluoride gave faster discoloration. Overall, cyclodextrins were not stable under molecular sieve synthesis conditions thereby preventing any structure direction.

Even with degradation some inorganic reactions containing Me-O- $\beta$ -CD gave products with fewer impurities (AFX and VET). This was not observed for all products and  $\beta$ -CD did not show similar improvements. Therefore, Me-O- $\beta$ -CD addition in reactions containing adamantyl SDAs could be a useful technique to improve product purity.

#### 4.5: References

1. S. I. Zones, Y. Nakagawa, G. S. Lee, C. Y. Chen and L. T. Yuen, *Microporous and Mesoporous Materials* **21** (4–6), 199–211 (1998).
2. Y. Nakagawa, US Patent No. 5,271,922 (1993).
3. M. Yoshikawa, P. Wagner, M. Lovallo, K. Tsuji, T. Takewaki, C. Y. Chen, L. W. Beck, C. Jones, M. Tsapatsis, S. I. Zones and M. E. Davis, *Journal of Physical Chemistry B* **102** (37), 7139–7147 (1998).
4. I. Ogino and M. E. Davis, *Microporous and Mesoporous Materials* **67** (1), 67–78 (2004).
5. K. Tsuji, P. Wagner and M. E. Davis, *Microporous and Mesoporous Materials* **28** (3), 461–469 (1999).

6. A. Burton, S. Elomari, C. Y. Chen, R. C. Medrud, I. Y. Chan, L. M. Bull, C. Kibby, T. V. Harris, S. I. Zones and E. S. Vittoratos, *Chemistry—a European Journal* **9** (23), 5737–5748 (2003).
7. C. C. Freyhardt, M. Tsapatsis, R. F. Lobo, K. J. Balkus and M. E. Davis, *Nature* **381** (6580), 295–298 (1996).
8. M. E. Davis and M. E. Brewster, *Nature Reviews Drug Discovery* **3** (12), 1023–1035 (2004).
9. M. E. Davis, C. Saldarriaga, C. Montes, J. Garces and C. Crowder, *Zeolites* **8** (5), 362–366 (1988).
10. A. Corma, M. J. Diaz-Cabanas, J. L. Jorda, C. Martinez and M. Moliner, *Nature* **443** (7113), 842–845 (2006).
11. C. T. Kresge, M. E. Leonowicz, W. J. Roth, J. C. Vartuli and J. S. Beck, *Nature* **359** (6397), 710–712 (1992).
12. S. L. Burkett and M. E. Davis, *Chemistry of Materials* **7** (8), 1453–1463 (1995).
13. A. Corma, F. Rey, J. Rius, M. J. Sabater and S. Valencia, *Nature* **431** (7006), 287–290 (2004).
14. F. Delprato, L. Delmotte, J. L. Guth and L. Huve, *Zeolites* **10** (6), 546–552 (1990).
15. S. L. Burkett and M. E. Davis, *Microporous Materials* **1** (4), 265–282 (1993).
16. E. W. Valyocsik, US Patent No. 5,670,131 (1997).
17. D. F. Shantz, A. Burton and R. F. Lobo, *Microporous and Mesoporous Materials* **31** (1–2), 61–73 (1999).
18. J. Tellinghuisen, *The Journal of Physical Chemistry B* **109** (42), 20027–20035 (2005).

19. M. J. Blandamer, P. M. Cullis and J. Engberts, *Journal of the Chemical Society-Faraday Transactions* **94** (16), 2261–2267 (1998).
20. P. Wagner, Y. Nakagawa, G. S. Lee, M. E. Davis, S. Elomari, R. C. Medrud and S. I. Zones, *Journal of the American Chemical Society* **122** (2), 263–273 (2000).
21. S. I. Zones, S. J. Hwang and M. E. Davis, *Chemistry—a European Journal* **7** (9), 1990–2001 (2001).
22. M. A. Camblor, C. Corell, A. Corma, M.-J. Diaz-Cabanas, S. Nicolopoulos, J. M. Gonzalez-Calbet and M. Vallet-Regi, *Chemistry of Materials* **8** (10), 2415–2417 (1996).
23. M. Yoshikawa, S. I. Zones and M. E. Davis, *Microporous Materials* **11** (3–4), 127–136 (1997).
24. S. I. Zones, *Journal of the Chemical Society-Faraday Transactions* **87** (22), 3709–3716 (1991).
25. S. I. Zones, S. J. Hwang, S. Elomari, I. Ogino, M. E. Davis and A. W. Burton, *Comptes Rendus Chimie* **8** (3–4), 267–282 (2005).
26. M. A. Camblor, M. J. Diaz-Cabanas, J. Perez-Pariente, S. J. Teat, W. Clegg, I. J. Shannon, P. Lightfoot, P. A. Wright and R. E. Morris, *Angewandte Chemie International Edition* **37** (15), 2122–2126 (1998).
27. In *Verified Syntheses of Zeolitic Materials*, edited by H. Robson and K. P. Lillerud (Elsevier Science B.V., 2001).
28. L. T. Yuen and S. I. Zones, Patent No. 20060115422 (2006).
29. R. H. Daniels, G. T. Kerr and L. D. Rollmann, *J. Am. Chem. Soc.* **100** (10), 3097–3100 (1978).

30. R. D. Shannon, *Acta Crystallographica Section A* **32** (SEP1), 751–767 (1976).
31. M. A. Camblor, M. Yoshikawa, S. I. Zones and M. E. Davis, in *Synthesis of Microporous Materials: Zeolites, Clays, Nanocomposites* (Marcel Dekker, New York, 1996), pp. 243.
32. M. J. Annen, M. E. Davis, J. B. Higgins and J. L. Schlenker, *Journal of the Chemical Society-Chemical Communications* (17), 1175–1176 (1991).
33. C. C. Freyhardt, R. F. Lobo, S. Khodabandeh, J. E. Lewis, M. Tsapatsis, M. Yoshikawa, M. A. Camblor, M. Pan, M. M. Helmkamp, S. I. Zones and M. E. Davis, *Journal of the American Chemical Society* **118** (31), 7299–7310 (1996).
34. S. I. Zones and S.-J. Hwang, *Microporous and Mesoporous Materials* **58** (3), 263–277 (2003).